



DIGITAL IMAGE CORRELATION TECHNIQUE IN MEASURING DEFORMATION AND FAILURE OF COMPOSITE AND ADHESIVE

Ab Ghani A. F

Sustainable Maintenance Engineering Research Group, Universiti Teknikal Malaysia Melaka, Malaysia
Faculty of Mechanical Engineering, Universiti Teknikal Malaysia Melaka, Durian Tunggal, Melaka, Malaysia
E-Mail: ahmadfuad@utem.edu.my

ABSTRACT

Digital image correlation technique is a non-destructive testing (NDT) tool for measuring deformation and failure of material have been used in this study over conventional methods such as strain gauges and extensometer. ASTM and other institutions have developed specific standards for composites. In the aim to inform the developed models of finite element/numerical and analytical, tensile tests were conducted on composite adherent and polymer adhesive specimens to obtain the stiffness and strengths of all constituents. Materials used for the testing campaigns are Glass Fiber Reinforced Polymer (GFRP) and Carbon Fiber Reinforced Polymer (CFRP) as well as adhesive materials for bulk testing Araldite 2015 and Sikaflex 292. The digital image correlation (DIC) technique is utilized for the characterisation of the constitutive and failure behaviour of the constituent materials, with focus on the composite and polymer adhesive material system.

Keywords: digital image correlation, GFRP/CFRP characterization, adhesive strain measurement, araldite, sikaflex.

INTRODUCTION

Advanced composite materials have been widely used due to their lightweight and high corrosion resistance. The composite structures are used in the various applications namely aerospace, automobiles, architecture, marine etc. It has attracted attentions in the past decades for improvement and optimisation issues. ASTM and other institutions have developed specific standards for composites. [1] In the aim to inform the developed models of finite element/numerical and analytical, tensile tests were conducted on composite adherent and polymer adhesive specimens to obtain the stiffness and strengths of all constituents. Materials used for the testing campaigns are Glass Fiber Reinforced Polymer (GFRP) and Carbon Fiber Reinforced Polymer (CFRP) as well as adhesive materials for bulk testing (Araldite 2015). Measuring strain has always been an important part of experimental mechanics, and is used extensively in analysing the properties of composite materials. The strain gauge was amongst the first methods of successfully obtaining strain data experimentally. Other methods were later discovered that focussed analysis on a more microscopic scale such as Atomic Force Microscopy (AFM), Scanning Electron Microscopy (SEM), and Computed Tomography (CT) [2].

MATERIALS

The GFRP prepreg a Unidirectional MTM28-1/1062-200-32%RW 300MM wide, with 0.16mm thickness after curing. The unidirectional prepreg GFRP is based on 120° C curing toughened, epoxy matrix resin, that have been specifically developed for the manufacture of components requiring high damage tolerance. The CFRP is unidirectional prepreg and it is MTM58FRB STS(24K) 36% RW with thickness after curing which is 0.45mm. Apart from that, structural adhesive namely Araldite 2015 and Sikaflex 292 also being tested using the

Universal Testing Machine and DIC as means of computing deformation.

DIGITAL IMAGING CORRELATION (DIC)

Introduction to digital imaging correlation (DIC)

Historically, DIC first came about in the 1980's due to the dawn of digital camera that had the 'processing power of a personal computer' [3]. It was the use of a digital camera that separated DIC from other experimental techniques that were employed to measure strain deformation. DIC has the ability to record images of deformed surfaces, allowing for accurate analysis of the material being stressed under load. Digital Image Correlation is a non-contact, optical method which captures of digital images of a surface of an object then performs the image analysis to obtain full-field deformation and measurements. This can be achieved by creating different methods like dots, grids, lines etc, on the specimen surface. The qualities of the results are mainly dependant on two factors: resolution of the camera, and quality of the speckle pattern on the specimen. DIC has developed into 3 main subsections of imaging. The first being 2D DIC, which measures in-plane deformation (x and y components). Secondly, there is 3D DIC, which also takes into account out-of-plane displacements, analysing data in the x, y, and z directions. Finally, there is V-DIC which determines measurements within a volume [3]. The strain distribution can then be obtained by applying the derivatives in the displacement field. To apply this method, the object under study needs to be prepared with random dot pattern speckle pattern to its surface.

Basic principles behind DIC

The concept of correlation is used to calculate the strains from the deformation of specimen. By observing



the speckle pattern of the image before and after the loading, comparisons can be made. The image is split up into a grid made from small subsets. It is the position of these co-ordinates before and after deformation that allows correlation to take place and to calculate strains from the imaging process.

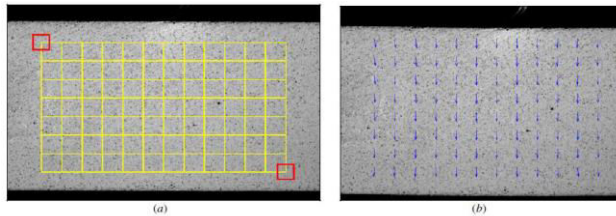


Figure-1. Reference image shows preview of grid co-ordinated display (b) shows displacement vectors of each co-ordinate point [4].

Figure-1 shows the correlation method allowing the user to determine the deformations of the sample. The two red squares pin pointed on the surface of the material is applied to track the motion of the centre point. The yellow grid is used to distinguish displacement fields. These changes are tracked during the experiment, and are then shown as vectors in (b) [4]. Assuming 2D-DIC, before a load has been applied it can be assumed that the co-ordinates that will be tracked can be denoted as (x_p, y_p) . After loading, the new co-ordinates can be denoted as (x_p', y_p')

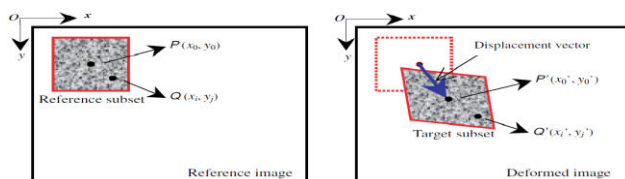


Figure-2. Shows the co-ordinate system before and after loading within the subset [4].

Figure-2 shows the reference subset before deformation occurs, and the target subset after loading. It can be seen that (x_p, y_p) is the subset centre from which other points such as (x_q, y_q) can be referenced to. The deformed image shows the position of these co-ordinates after loading, and using subset matching, can be correlated back to the un-deformed image. The following equations are used within computing algorithms to calculate deformed positions with relation to the previous co-ordinates [5]:

$$x_q' = x_q + u_p = \frac{\partial u_p}{\partial x} \Delta x_q + \frac{\partial u_p}{\partial y} \Delta y_q \quad (1)$$

$$y_q' = y_q + v_p = \frac{\partial v_p}{\partial y} \Delta y_q + \frac{\partial v_p}{\partial x} \Delta x_q \quad (2)$$

Where up and vp are the x and y components of the displacement vector point p. Accordingly, xq and yq

are the co-ordinates of q prior to loading [5]. These equations are just simple equations which describe the mathematical location of the co-ordinates after deformation.

MATERIAL PROPERTIES EXTRACTION TESTING

Tensile testing

Material properties for adherends and adhesive bulk coupon are extracted from a tensile test method as per ASTM using Instron E Testing Equipment. Measurement of E_{11} , E_{22} , ν_{12} , and ν_{21} and Tensile Strength were obtained from the uniaxial tensile test. Strain gauges and DIC method were used to measure strain while stress were computed using cell load from tensile test. Biaxial strain gauge were bonded onto the side of specimen to measure the in-plane strains and poisson ratio.

Type of machine used: Instron E, Instron F and Instron C universal testing machine

Variables Measured: Displacement load and strain using strain gauges and Digital Image Correlation (DIC)

Tensile Properties such as lamina's Young Modulus E_1 and E_2 , Poisson's ratio and lamina longitudinal and transverse tensile strength are measured by static tension testing along 0 degree and 90 degree according to the ASTM D3039 standard test method. The test specimen is given in the figure below. Table-1 shows its dimension for 0 degree uniaxial tensile test coupon

Table-1. Tensile test coupon dimension for FRP (0 degree).

Section	Dimension (mm)
Length	250
Width	15
Thickness	1
Tab Length	56
Tab Thickness	1.5

The tensile specimen was placed in a testing machine aligning the longitudinal axis of the specimen and pulled at a crosshead speed of 2 mm/min. The specimens were loaded step by step till they fail under uniaxial loading. The load was recorded using the digital data acquisition system. The axial and the transverse strains were obtained by a pair of two linear strain gauges, which were attached to the gage section of the specimen. The stress strain behaviour is obtained to be linear and the final failure occurs catastrophically. The values of young's modulus, poisons ratio and axial strength are obtained as follows:

$$\sigma_1 = \frac{P}{A} \quad \nu_{12} = -\frac{\varepsilon_1}{\varepsilon_2} \quad E_1 = \frac{\sigma_1}{\varepsilon_1} \quad X_t = \frac{P_{ult}}{A} \quad (3)$$



The transverse young's modulus minor poisons ratio and transverse tensile strength are calculated from the tension test data of 90 degree unidirectional lamina. The tension test is manufactured based on the ASTM 3039 standards and the specimen dimensions are given in the figure below. Table-2 shows its dimension.

Noise and errors assumption

In particular, it is assumed the use of modern, charge-coupled device (CCD) cameras where photons produce electrons that are commonly referred to as photoelectrons. Local filtering will be hard for the noise will be hard to execute where measuring will change throughout the test, i.e. local error from CCD noise (the random movement/changes in grey level) will change throughout the test depending on the pattern/the lighting/the deformation/the location. It is more common to evaluate a global value of strain error by taking a series of ~20 images (over a suitable length of time/frame rate similar to the test) of the speckled specimen, with the test lighting, with no load, i.e. stationary. Before the

measurement of strain is taken from DIC system, it is required to measure the strain at no load condition as means of computing the level of noise and resolution. The standard deviation was computed for strain at no load condition, and this will be measure of resolution of the measurement. The images of noise computation is as shown in Figure-4.

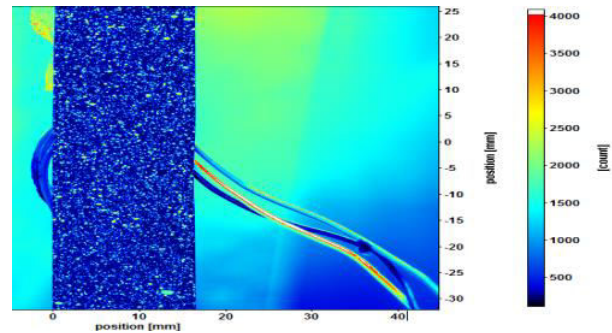


Figure-3. GFRP 0 degree uniaxial tensile test.

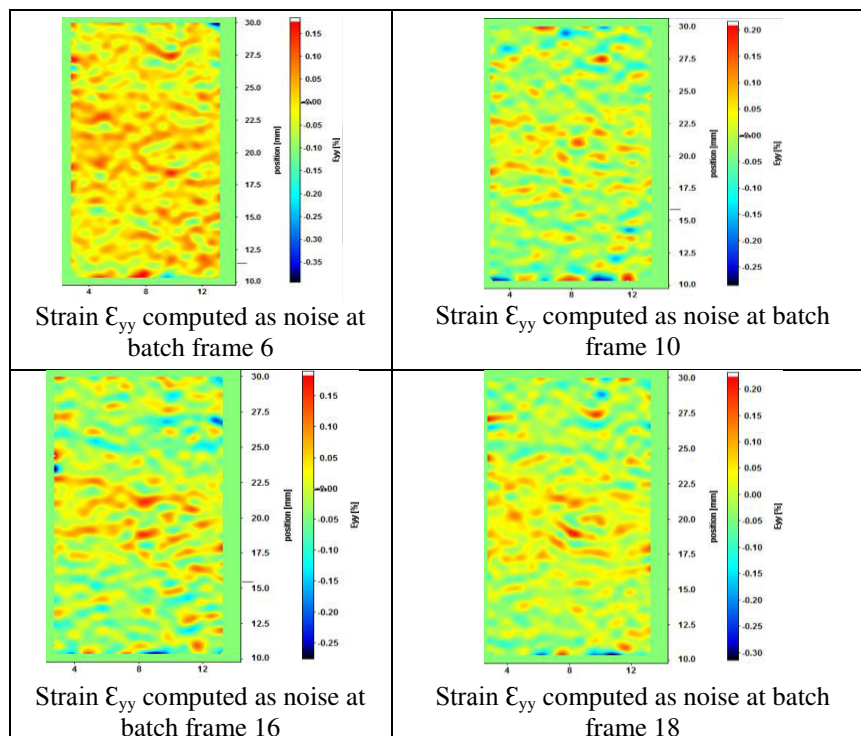


Figure-4. Noise strain, ϵ_{yy} contour at batch frame 6, 10, 16 and 18 of no load condition.

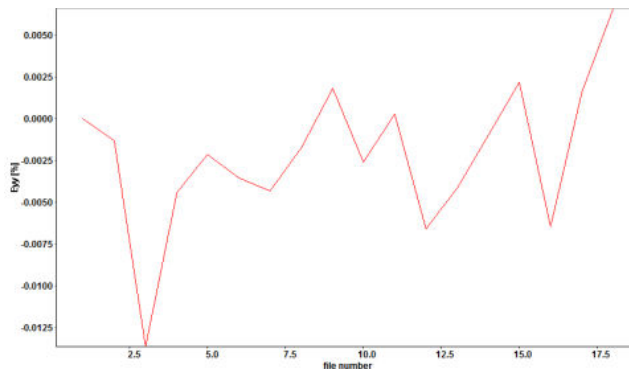


Figure-5. No load strain measurement (noise) for 0 degree CFRP sample 1.

- Standard deviation of $3.26649E^{-05}$
- Mean $3.57795E^{-05}$

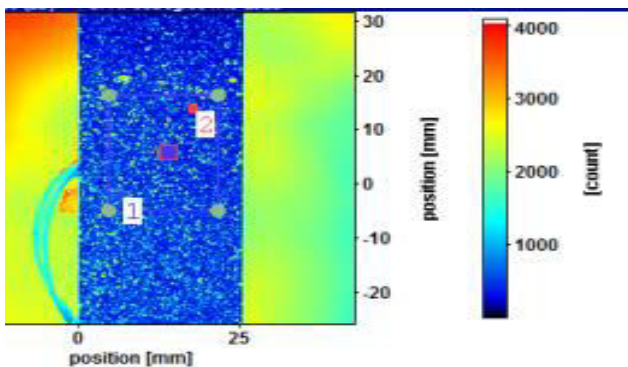


Figure-6. Gauge region for CFRP 90 degree tensile test.

Strain measurement region was taken at the location where the strain gauges are attached on the other side of specimen to aim for matching measurement taken from DIC and strain gauges. The approximate area of 20mmX10mm was measured as to avoid the edge effect on the strain computation as shown in Figure-6. The region was scoped to about 3 mm off the edge at either side. As accordance to ASTM D3039 description, < 3 to 5% bending considered good testing practice due to the fact that it has been generally shown that over 5% bending decreases ultimate failure strength. In these tests, the strain computation from both side of the specimens are taken using strain gauges at one side and digital image correlation technique on the other.

Failure mode for 90 degree UD GFRP and CFRP

All the four samples of 90 degree UD GFRP and four samples of 90 degree CFRP showed similar failure pattern which were breakage at matrix region with neighbouring fiber. It was found that transverse cracking initiated and propagate through the matrix and interface. [6] This cracking occurred through the weak fibre/matrix interface and also happened through the matrix epoxy resin. The stress strain plot for the transverse UD GFRP

and UD CFRP shown a little non linearity at the end of the plot approaching the failure load. Variations in mechanical properties were lower than 10% so results are considered good for 0 degree UD GFRP and 0 degree UD CFRP in terms of young modulus E_{11} and Tensile Strength. Slight variation in terms of Tensile Strength for GFRP and CFRP 90 degree were obtained among the samples, while Transverse Modulus of elasticity shows consistency.

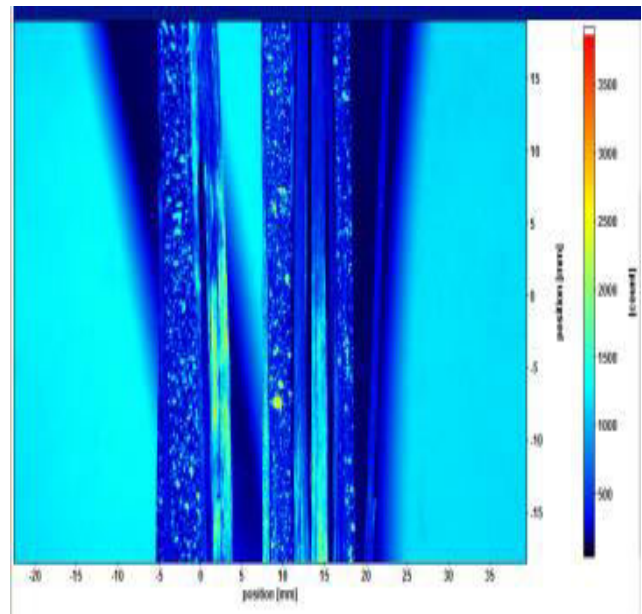


Figure-7. CFRP 0 degree uniaxial sample 1 when it break at 43452N.

The Figure-7 shows the captured image of the 0 Degree Unidirectional CFRP when it breaks. It is shown that DIC is able to aid in detecting mode of failure as well as strain to failure of CFRP under longitudinal tensile loading. Figure-8 depicts the contour of displacement in y direction (load direction) where it is expected uniform contour with respect to region near the area where loading is applied (gripping section) experiencing higher displacement contour as compared to the middle section of the tensile coupon. Meanwhile for Figures 9(a), (b) and (c) shows plot obtained from DIC method for strain in yy direction of CFRP 0 degree UD. The plot of stress in yy direction is plotted against strain in yy direction in order to extract the material properties of Modulus of Elasticity in y direction, E_1 . Results obtained compares well with reported in manufacturer's data sheet. Measurement using DIC and strain gauges also in agreement with each other showing the consistency of this method with conventional method. The strain gauges however sometime could not measure strain upto to failure point due to slippery surface and deformation behaviour of the samples. Hence by using DIC, interpolation is not needed to capture strain to failure.

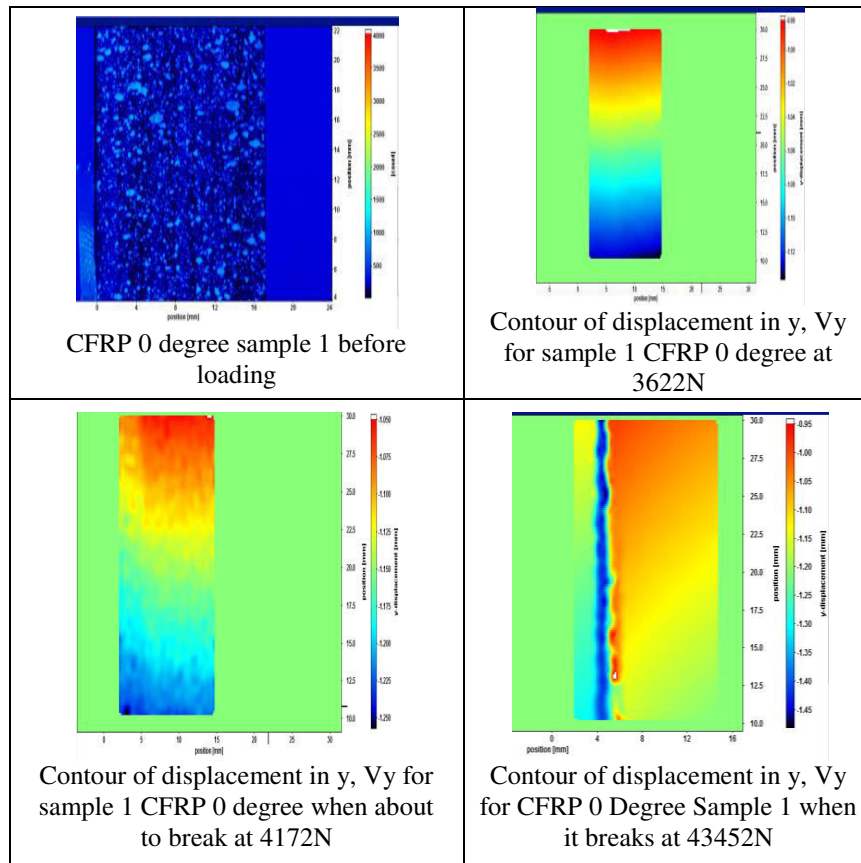


Figure-8. Contour of displacement, Vy for sample 0 degree CFRP.

CFRP 0 degree unidirectional uniaxial tensile testing

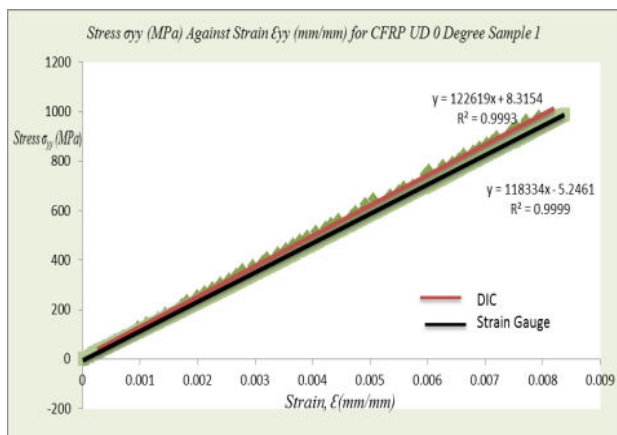


Figure-9(a). Stress against strain plot for sample 1 CFRP 0 degree UD.

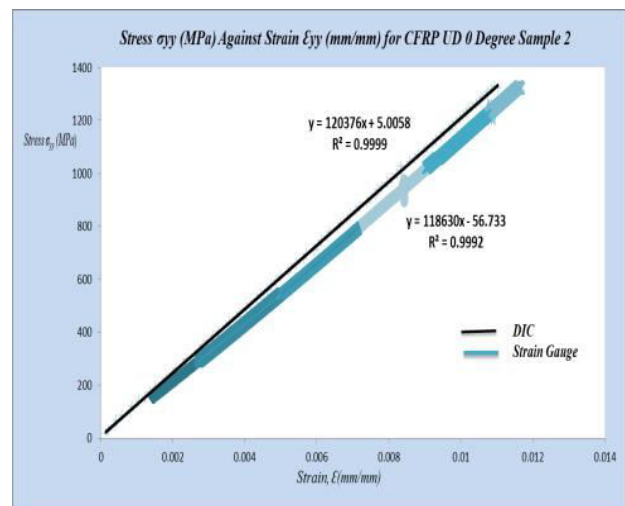


Figure-9(b). Stress against strain plot for sample 2 CFRP 0 degree UD.

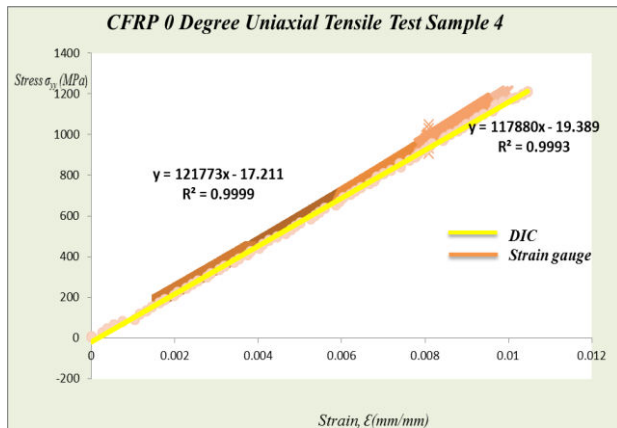


Figure-9(c). Stress against strain plot for sample 4 CFRP 0 degree UD.

GFRP 0 degree unidirectional uniaxial tensile testing

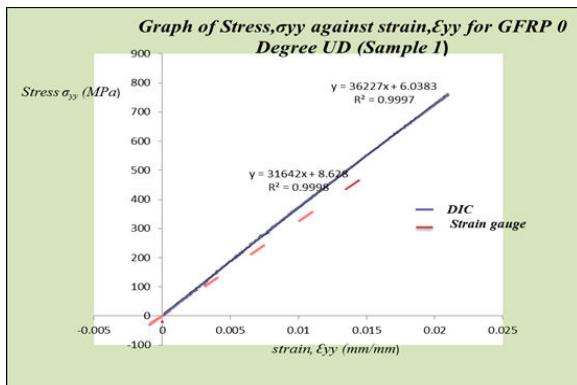


Figure-10(a) Stress against strain plot for sample 1 GFRP 0 degree UD.

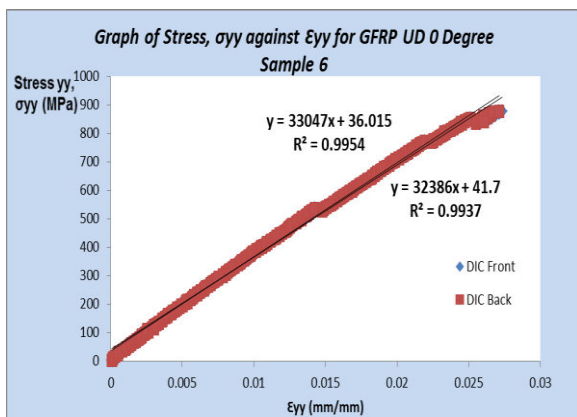


Figure-10(b). Stress against strain plot for sample 6 GFRP 0 degree UD.

Summary of experimental results for UD 0 degree GFRP/CFRP and UD 90 Degree GFRP/CFRP

Table-2(a). GFRP 0 degree UD.

	E_{11} (MPa)	Tensile Strength (MPa)	ν_{12}
Sample 1	36031	791.69519	0.306
Sample 2	37346	875.5965	0.28379
Sample 3	38059	881.8734177	0.28759
Sample 4	37328	898.4810127	0.29074
Sample 5	32716	882	0.29

Table-2(b). CFRP 0 degree UD.

	E_{11} (MPa)	Tensile Strength (MPa)	ν_{12}
Sample 1	122619	1211	0.31
Sample 2	120376	1322	0.31
Sample 3	110913	1337	NA
Sample 4	117880	1172	0.3

Table-2(c). GFRP 90 degree UD.

	E_{22} (MPa)	Tensile Strength (MPa)
Sample 1	8852.9	68.6
Sample 2	10459	60.6
Sample 3	10173	60.3
Sample 4	10132	62.1

Table-2(d). CFRP 90 degree UD.

	E_{22} (MPa)	Tensile strength (MPa)
Sample 1	7669	16.1
Sample 2	7993.2	15.9
Sample 3	7630.5	24.51
Sample 4	7256.3	15.67

DIC deformation and failure computation for Araldite 2015 and Sikaflex 292

Deformation behaviour and failure also being computed by the DIC method on structural adhesive Araldite 2015 (brittle) and Sikaflex 292 (ductile/flexible). Araldite 2015 is a two component epoxy paste adhesive. It is a toughened paste which is suitable for bonding GRP, SMC and dissimilar substrates. It has low shrinkage and gap filling as well as exhibit non sagging up to 10mm thickness as accordance to its manufacturer's data sheet. Setting used for tensile testing of Araldite 2015 was the same for GFRP/CFRP uniaxial tensile testing using universal testing machine with 2mm/min displacement crosshead. The Araldite 2015 was tested in uniaxial tensile test as accordance to ASTM D638 Tensile Properties of Plastics. Mould made of silicone is used to form adhesive bulk testing coupon as per dimension described in Table-3.



Table-3. Dimension of adhesive bulk testing specimen for uniaxial tensile.

Section	Dimension (mm)
Length	225
Width	19
Thickness	4
Dog bone end length	60
Dog bone end width	30

Subset size of 31X31 and step size of 8 is taken after parametric study of varying the subset size influence on the measurement strain shown that the value not differ significantly each other as per shown below. The difference is about **0.01%** with each other.

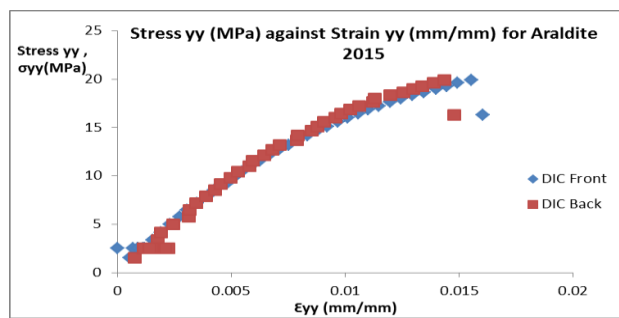


Figure-11. Stress against strain plot for Araldite 2015 sample 4.

Table-4. Araldite 2015 mechanical properties uniaxial test.

	E_{11}/E_{22} (MPa)	Tensile strength(MPa)	ν_{12}/ν_{21}
Sample 1	1376	18	0.35
Sample 2	2562	18.63	0.34
Sample 3	2471	24.49	0.34
Sample 4	1430	20	0.337
Sample 5	1637	15	0.34

The deformation of structural adhesive Araldite 2015 shows deformation and behaviour of elastic upto brittle point where sudden break occur. This is expected due to the fact that it is an epoxy based material with similar constituent as in composite material of epoxy as resin. The DIC method is able to capture the deformation of elastic regime upto failure point successfully which results in ability to get the failure strain and match with the tensile strength recorded from load cell. The value of modulus of elasticity of Araldite 2015 obtained in the tensile test, 1.895GPa is also in agreement and close with reported elsewhere [7] which is 1.85GPa. The measurement were tabulated in Table-4.

Sikaflex 292 (Ductile/Flexible)

Sikaflex 292 is a non sag one component polyurethane adhesive of thixotropic, paste-like consistency which cures on exposure to atmospheric moisture to form a durable elastomer. Sikaflex 292 exhibits excellent adhesive properties and a high degree of mechanical strength. The material Sikaflex 292 is prepared for uniaxial tensile testing in the form of dog bone shape.

Material testing

As accordance to the material data sheet provided for Sikaflex 292, it is shown that tensile strength is (DIN 53504) 4 N/mm² approximately. As in this research the testing of the specimen using different standard which is ASTM D412, it is expected that some variation in strength will occur. The stress needed to break the sample is the tensile strength of the material is Tensile Strength. 5 specimens were tested as per ASTM D412. The sample is as shown in Figure-12. It was obtained that the Tensile Strength obtained were in the range of 1.43N/mm² to 1.6 MPa. The Modulus of Elasticity, E was obtained to be of magnitude 5.4 MPa. There was no reported value of Modulus of Elasticity given in the material data sheet. As for elongation at break as stated in the material data sheet is; Elongation at break (DIN 53504) > 300%. It was in agreement with the results obtained from uniaxial tensile test perform on Sikaflex 292 where it exhibit elastic plastic deformation which recorded the elongation at break around 0.45~0.53. Figure 13 shows the large elongation exhibited by Sikaflex.



Figure-12. Sikaflex 292 curing at ambient temperature for 3 days.



Figure-13. Sikaflex 292 behaving elastic plastic deformation.

The hardening curve data are required in the tabular form of yield stress with plastic strain where the first pair of numbers must correspond to the initial yield stress at zero plastic strain in order to plot for elastic plastic material modelling in Abaqus software.

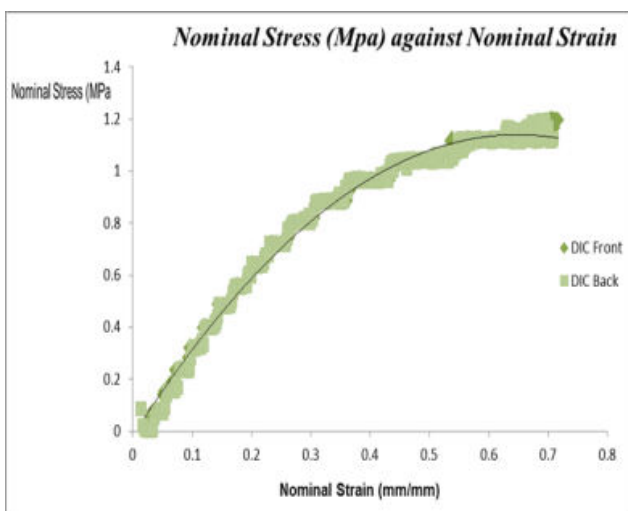


Figure-14 (a). Sample 3 Sikaflex 292 nominal stress against nominal strain.

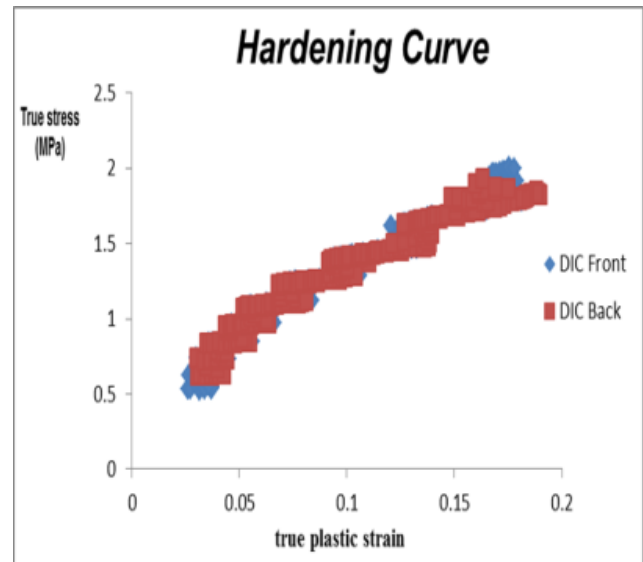


Figure-14(b). Sample 3 Sikaflex 292 hardening curve.

Figures 14(a) and 14(b) are nominal stress and strain plot as well as hardening curve after extracted strain measurement from DIC and true stress computation and true strain computation based on elastic plastic behaviour.

Failure mode of Sikaflex 292



Figure-15. Sikaflex 292 after ruptured/failure.

It experienced deformation elastically surpassing the yield point then undergoing plastic region, strain hardening, necking and stress concentration magnified in the necking area making the sample ruptured as it enabled to hold any load at its ultimate tensile strength.

Different in deformation between Araldite 2015 and Sikaflex 292

It takes a lot of force to break brittle adhesive material Araldite 2015 but not much energy as there small area underneath the curve of stress strain as compared to ductile material such as Sikaflex 292. Araldite 2015 could not stretch very far before it breaks. A material like this which is strong, but unable to deform very much before it ruptured. The ductile sample (Sikaflex 292) elongates a lot



more before breaking than the brittle sample (Araldite 2015) does. Deformation allows a sample to dissipate energy. If a sample unable to deform any longer the energy will not be dissipated and the sample will rupture. [9]

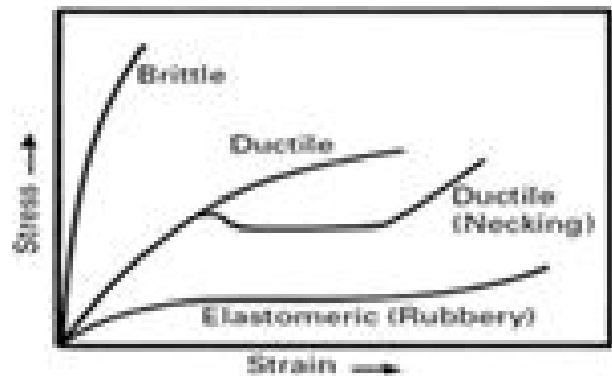


Figure-16. Deformation for different nature of adhesive type.

Table-5. Sikaflex 292 mechanical properties extraction.

	E_{11}/E_{22} (MPa)	Tensile strength (MPa)	ν_{12}/ν_{21}	Strain to failure
Sample 1	5.465	3.2	0.31	0.016
Sample 2	4.45	3	0.315	0.01
Sample 3	2.3	3.4	0.31	0.012
Sample 4	2.68	3	0.31	0.015
Sample 5	3.28	3.2	0.312	0.012
Mean	3.64	3.16	0.311	0.013
Std Dev	1.17	0.15	0.0019	0.0022

Correlation technique for deformation computation on Araldite 2015 and Sikaflex 292

During simulation of Digital Image Correlation (DIC) using Davis 8, several parameters have been tested in regards of the factors affecting the computation of strain for polymeric based material such as Sikaflex 292. Parametric study on the subset size influence on the strain computation, ϵ_{yy} had been performed. It is seen that the relation of subset size chosen on the strain computation proved that it has insignificant effect on strain yy computation.

The setting for DIC on commercial software for computation of strain in yy and strain xx direction for uniaxial tensile test of Araldite have been set using same setting as per the uniaxial tensile testing of GFRP 0 degree UD/GFRP 90 degree UD and CFRP 0 degree UD/CFRP 90 degree UD where it was found that by parametric study on subset size and step size, the setting of 41 subset size and 12 step size obtained consistent and converge results in terms of strain yy and strain xx computation. Therefore, considering similar deformation shown by Araldite 2015 of elastic brittle deformation, same setting and parameter for DIC calculation are used. Meanwhile for Sikaflex 292, the elastic plastic deformation experienced by the material requesting different type of computation for DIC since it involves large strain. As for computation setting for DIC involves two different displacement calculation and correlation algorithm which suit different material

behaviour. As for elastic brittle material, the use of "Relative to first" is used. It involves the setting of the deformation of each image is determined relatively to the first image of the sequence.

On the other hand, for elastic plastic behaviour which involves high deformation such as Sikaflex 292, it is recommended and practical to use method in DIC of; "Sum of differential" where the deformation of each image is the sum of differential of the preceding images. This way of following the movement over time is equivalent to "relative to first" and works even for large deformation over time or if lighting conditions change. The drawback is a lower precision the calculation errors will sum up as well as the measured deformation. The noise goes up with the square root of number of images. Higher value of "max expected deformation" has been selected considering finding seeding points in subsequent images where large deformation has occurred but is result in a higher computation time than normal. [8]

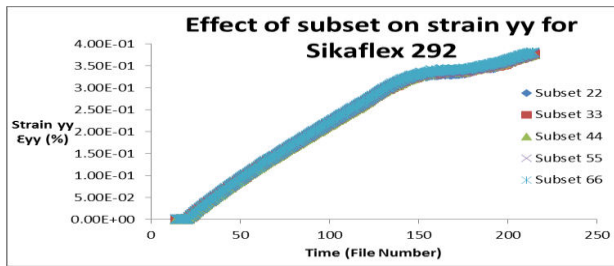


Figure-17. Effect of subset size variation on computation of strain.

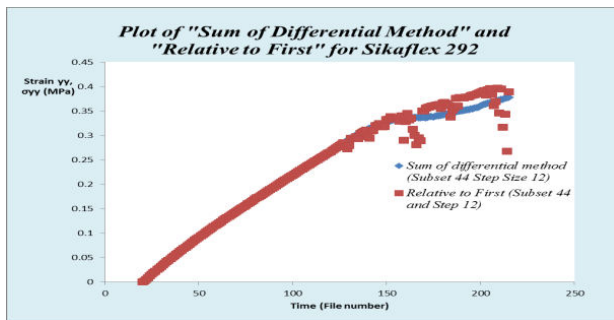


Figure-18. Sum of differential method and relative to first technique for strain measurement.

Figure-17 shows the effect of subset size variation on computation where no noticeable difference is seen with respect to subset size. Meanwhile, the method of correlation is significant in measuring strain for high deformation material such as Sikaflex 292 where Figure-18 shows that at higher strain, the difference between relative to first and sum of differential is obvious. This occurred due to large elongation experienced by the material under tensile loading.

CONCLUSIONS

Digital image correlation technique had been performed to measure deformation in terms of displacement and strain for GFRP, CFRP, Araldite and Sikaflex. Tensile testing had been performed based on ASTM standard and computation of strain and mechanical properties of each constituent had been extracted with comparison with strain measured using strain gauges. DIC had been proven able to get similar values of Modulus of Elasticity for Araldite 2015 reported elsewhere and this method is very suitable to be applied on the surface of adhesive materials while strain gauges will need fine surface preparation and bonded mechanism to attach onto. Two different methods of correlation had been used to measure the strain for material Sikaflex 292 which experiences large deformation and the sum of differential has been the effective method to measure deformation for large strain material.

REFERENCES

- [1] U.S. Department of Defense, MIL-HDBK-17-1F. Composite Materials Handbook, Volume 1 Chapter 7
- [2] Vishay Precision Group, Plane-Shear Measurement with Strain Gages, Tech Note TN-512-1 Strain Gages and Instruments
- [3] P. Reu, "Introduction to Digital Imaging Techniques," Experimental Techniques, pp. 3-4, 2012.
- [4] B. Pan, K. Qian, H. Xie and A. Asundi, "Two-dimensional image correlation for in plane displacement and strain measurement: a review," Measurement Science and Technology, 2009.
- [5] T. A. Berfield, J. K. Patel, R. G. Shimmin, P. V. Braun, J. Lambros and N. R. Sottos, "Micro- and Nanoscale Deformation Measurement of Surface and Internal Planes via Digital Image Correlation," Experimental Mechanics (2007) 47: 51-62.
- [6] Donald F. Adams, Leif A. Carlsson, R. Byron Pipes, Experimental Characterization of Advanced Composite Materials, CRC Press. CRC Press, Oct 29, 2002
- [7] R. D. S. G. Campilho, M. D. Banea, J. A. B. P. Neto, L. F. M. da Silva, Modelling of Single-Lap Joints Using Cohesive Zone Models: Effect of the Cohesive Parameters on the Output of the Simulations, The Journal of Adhesion Volume 88, Issue 4-6, 2012, pages 513-533
- [8] Zhengzong Tanga, Jin Lianga, Zhenzhong Xiaoa, b, Cheng Guoa, Large deformation measurement scheme for 3D digital image correlation method, Optics and Lasers in Engineering Volume 50, Issue 2, February 2012, Pages 122-130
- [9] A.T. Nettles, Basic Mechanics of Laminated Composite Plates NASA Reference Publication 1351, 1994.